ACS Medicinal Chemistry Letters
Cite This: ACS Med. Chem. Lett. 2019, 10, 504−510
Letter
pubs.acs.org/acsmedchemlett

Investigation around the Oxadiazole Core in the Discovery of a New Chemotype of Potent and Selective FXR Antagonists

Carmen Festa,[†] Claudia Finamore,[†] Silvia Marchianò,[‡] Francesco Saverio Di Leva,[†] Adriana Carino,[‡] Maria Chiara Monti,[∥] Federica del Gaudio,[∥] Sara Ceccacci,[∥] Vittorio Limongelli,[†,§] Angela Zampella,[†] Stefano Fiorucci,[‡] and Simona De Marino*[,†]

[†]Department of Pharmacy, University of Naples "Federico II", Via D. Montesano 49, Naples 80131, Italy
[‡]Department of Surgery and Biomedical Sciences, Nuova Facoltà di Medicina, Perugia 06132, Italy
[§]Faculty of Biomedical Sciences, Institute of Computational Science - Center for Computational Medicine in Cardiology, Università della Svizzera italiana (USI), Via G. Buffi 13, Lugano CH-6900, Switzerland
[∥]Department of Pharmacy, University of Salerno, Via Giovanni Paolo II, 132, Fisciano, Salerno 84084, Italy

S *Supporting Information*

ABSTRACT: Recent findings have shown that Farnesoid X Receptor (FXR) antagonists might be useful in the treatment of cholestasis and related metabolic disorders. In this paper, we report the discovery of a new chemotype of FXR antagonists featured by a 3,5-disubstituted oxadiazole core. In total, 35 new derivatives were designed and synthesized, and notably, compounds **3f** and **13**, containing a piperidine ring, displayed the best antagonistic activity against FXR with promising cellular potency (IC_{50} = 0.58 ± 0.27 and 0.127 ± 0.02 μM, respectively). The excellent pharmacokinetic properties make compound **3f** the most promising lead identified in this study.

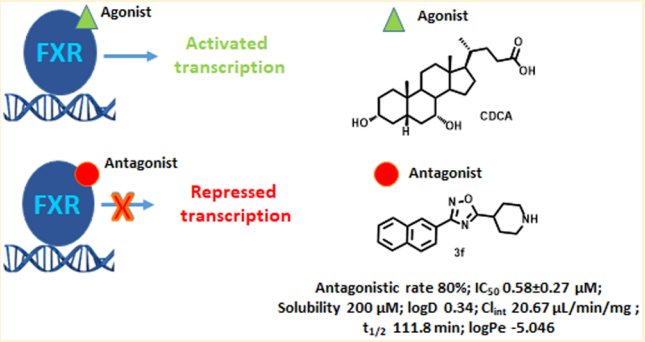

KEYWORDS: *FXR antagonists, bile acid receptor, 1,2,4-oxadiazole core, piperidine ring, pyrrolidine ring*

Farnesoid X Receptor (FXR, also known as BAR, NR1H4), a ligand-dependent transcription factor, belongs to the superfamily of metabolic nuclear receptors. FXR is highly expressed in the liver, intestine, kidney, and adrenals, and it responds to bile acids[1] regulating their homeostasis and governing lipid and glucose metabolism in the liver.[2−6] For all these reasons, FXR represents a promising pharmacological target in the management of metabolic disorders.

The most potent endogenous ligand of FXR is chenodeoxycholic acid (CDCA), a primary bile acid found in human bile. FXR agonists bind to the FXR ligand binding activation function 2 (AF-2) domain (LBD) inducing a receptor conformational change responsible for the release of corepressor molecules (such as N-Cor) and the recruitment of coactivators (such as SRC-1). The FXR/coactivator complex assisted by the RXR protein binds to specific regions of DNA enhancing the expression of target genes. On the other hand, the binding of an antagonist molecule to the FXR-LBD induces a shift of AF-2 helix which assumes an orientation unable to recruit the coactivators, thus leading to transcriptional silencing.[7]

The strong interest toward FXR agonists is linked to the ability of these compounds in regulating bile acid homeostasis in cholestasis, lowering plasma lipogenesis, repressing very low density lipoprotein production, increasing plasma triglyceride clearance, improving insulin sensitivity, and promoting the storage of glycogen.[8,9]

In recent years, several FXR agonists, belonging to steroidal and nonsteroidal scaffolds, have been identified as potential leads for the treatment of metabolic disorders with some of them progressed in advanced clinical trials for the treatment of patients with primary biliary cirrhosis (PBC) and nonalcoholic steatohepatitis (NASH).[10] Unfortunately, the side effects resulted from the phase III clinical trials of 6-ECDCA, the most promising steroidal FXR agonist,[10] raised concerns about the use of FXR agonists in the treatment of metabolic liver diseases. In addition, the recent finding that the FXR gene ablation protects from liver injury caused by bile duct ligation (BDL) has moved the attention toward the FXR antagonism in the treatment of obstructive cholestasis.[11]

As in the case of the agonists, both steroidal and nonsteroidal compounds[12−14] have been identified as FXR antagonists. Among the steroidal scaffolds, the most promising are natural compounds with glyco-β-muricholic acid

Special Issue: Highlighting Medicinal Chemistry in Italy

Received: November 6, 2018
Accepted: January 8, 2019
Published: January 10, 2019

DOI: 10.1021/acsmedchemlett.8b00534
ACS Med. Chem. Lett. 2019, 10, 504−510

(GβMCA) currently in advanced preclinical trials for the treatment of obesity, NAFLD, and insulin resistance.[15] In this work, starting from the recent discovery of Flesch et al.[16] who showed that structural fragmentation on GW4064, a highly potent and selective nonsteroidal FXR agonist, can lead to the shift of the receptor modulation from the agonism to the antagonism, we aimed at developing novel nonsteroidal FXR antagonists. In particular, Flesch et al.[16] reported that the removal of the bulky 4-substituent from the isoxazole ring of GW4064 can be a valuable starting point for the synthesis of FXR antagonists. In detail, the replacement of the isoxazole ring in GW4064 with a 3,5-disubsituted oxadiazole led to compounds with different activity profiles, from agonism to partial agonism and antagonism.

The 1,2,4-oxadiazole ring is interesting from the chemical synthesis point of view, being an accessible and highly diversifiable scaffold that can be exploited to improve the pharmacokinetics, pharmacodynamics, and the selectivity profile of the drug candidates.

This is the case of compound **1** in Figure 1, a highly simplified GW4064 derivative endowed with an antagonistic profile toward FXR.

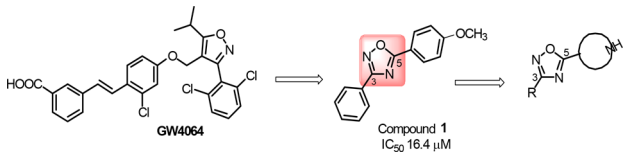

Figure 1.

Despite the promising pharmacological profile of **1**, a strong rationale of its activity, supported by the elucidation of the ligand binding mode, is lacking. Therefore, we have decided to explore further this scaffold, modifying both substituents at C-3 and C-5 of the oxadiazole moiety developing a small library of derivatives listed in Table 1. In particular, the lipophilic *p*-methoxyphenyl at C-5 in **1** was replaced by different protonable *N*-bearing heterocyclic substituents, such as a piperidine or a pyrrolidine ring. It is worth noting that a similar substituent has been recently reported by Teno et al.,[13] in a new chemotype of FXR antagonists with the evidence that the replacement of a cyclohexyl component with an ionizable piperidine ring increases the binding activity to FXR. The research of Teno et al. led finally to the identification of *N*-acylated electrically neutral potent FXR antagonists. At variance with the Teno's compounds, in our derivatives, the *N*-bearing ring is not acetylated and, hence, protonable, thus endowing basic properties to our compounds and allowing to explore the piperidine moiety as an available H-bond donor group in the FXR-LBD.

Here, we report the pharmacological evaluation, the assessment of the in vitro pharmacokinetic properties, and the ligand binding mode to FXR of the newly synthesized compounds that allowed the identification of novel potent FXR antagonists with promising pharmacokinetic properties.

The structure of the synthesized compounds was confirmed by spectroscopic and analytical techniques, and the structural characterization is available in the Supporting Information.

Synthesis started with oxadiazole derivatives **3a−f** prepared from the nitriles **1a−f** and *N*-Boc-isonipecotic acid (*N*-Boc-Inp-OH), as starting materials (Scheme 1).

Briefly, treatment of nitriles **1a−f** with hydroxylamine hydrochloride afforded the intermediate amidoximes **2a−f** in quantitative yield.

Reaction with *N*-Boc-isonipecotic acid (*N*-Boc-Inp-OH), using HBTU as coupling agent, followed by deprotection of the Boc protecting group in acidic conditions, led to compounds **3a−f** (Scheme 1). Compounds **3a−f** were evaluated in a luciferase reporter assay on HepG2 cells transiently transfected with human FXR (Table 1). None of the above resulting compounds were able to transactivate FXR in agonistic mode at 10 μM concentration (Figure S3) whereas cell costimulation in the presence of CDCA (10 μM) reveals that, among this series, derivative **3f** was relatively effective (80% antagonistic rate) in inhibiting FXR activation caused by CDCA, and the above efficacy data was accompanied by a promising potency (IC_{50} 0.58 ± 0.27 μM). Having identified the 3-naphtyl-1,2,4-oxadiazole as a promising core in FXR antagonism, substitutions preserving the naphtyl at C-3 and the protonable core at C-5 have been explored. First, compounds **13** and **23** have been prepared reacting the amidoxima **2f** with *N*-Boc-L-pipecolic acid (*N*-Boc-L-Pip-OH) and *N*-Boc-L-proline (*N*-Boc-L-Pro-OH) (Scheme 2), in order to explore the influence of different size and different position of the nitrogen in the heterocyclic moiety at C-5. Compound **13** was also demonstrated to be a high potent FXR antagonist (IC_{50} 0.127 ± 0.02 μM), whereas a dramatic loss of potency was observed for the corresponding proline derivative **23**, thus identifying the *N*-bearing six membered heterocycle as a key structural element at C-5 position on the central 1,2,4-oxadiazole moiety. Therefore, the effect of the introduction of *N*-alkyl side chain with differentiated lengths and functionalization has been the focus, using compounds **3f**, **13**, and **23** as cornerstone intermediates. *N*-Alkylation with β, γ, or δ-bromo esters, as depicted in Scheme 2, allowed the introduction of C-3/C-4 or C-5 side chains with the methyl ester end-group. Basic hydrolysis with LiOH and reduction with DIBAL-H afforded the corresponding acids and alcohols (Scheme 2).

Alkylation at the nitrogen affects FXR antagonism. As shown in Table 1, the effects in terms of efficacy/potency are highly dependent on the position of the nitrogen in the cycle, the length of the alkyl chain, and the nature of the terminal functional group (COOH or CH_2OH). Foremost, the introduction of alkyl side chains bearing a carboxylic group produces substantial changes in FXR antagonistic activity compared to nonalkylated counterparts, with a dramatic increase in IC_{50} values. Importantly, the above loss in potency is independent of the length of the *N*-alkyl chain and the position of the nitrogen on the heterocycle at C-5.

Of interest, the replacement of the carboxylic end group with a neutral alcoholic functional group preserves the antagonistic activity toward FXR. Furthermore, the biological activity indicates that the efficacy in antagonizing FXR correlates with the size of the installed side chain, with the best match found for the C-4 side chain as in compounds **9** and **19** (IC_{50} value of 1.17 and 7.0 μM, respectively). The comparison between the IC_{50} values of the *N*-alkylated piperidine derivatives with those of the *N*-free piperidine **3f** and **13** shows that the modification at the nitrogen atom alters the ligand potency, prompting the nonsubstituted piperidine ring as a key structural element in the FXR antagonism, with compounds **3f** and **13** being the best hits identified in this study.

DOI: 10.1021/acsmedchemlett.8b00534
ACS Med. Chem. Lett. 2019, 10, 504−510

Table 1. FXR Antagonistic Activity of Substituted 1,2,4-Oxadiazole Derivatives

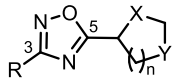

Compound	R	n	X	Y	Efficacy [%][a]	IC_{50}[b]
3a	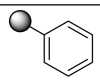	2	CH_2	NH	0	-
3b	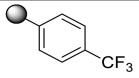	2	CH_2	NH	44	-
3c	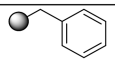	2	CH_2	NH	9	-
3d	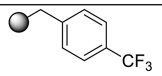	2	CH_2	NH	13	-
3e	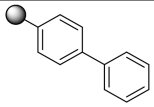	2	CH_2	NH	49	-
3f	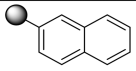 Naph	2	CH_2	NH	80	0.58±0.27 μM
5	Naph	2	CH_2	$N(CH_2)_2COOH$	19	-
6	Naph	2	CH_2	$N(CH_2)_2CH_2OH$	67	40.4±7.66 μM
8	Naph	2	CH_2	$N(CH_2)_3COOH$	74	25.7±1.69 μM
9	Naph	2	CH_2	$N(CH_2)_3CH_2OH$	95	1.17±0.41 μM
11	Naph	2	CH_2	$N(CH_2)_4COOH$	2	-
12	Naph	2	CH_2	$N(CH_2)_4CH_2OH$	48	-
13	Naph	2	NH	CH_2	96	0.127±0.02 μM
15	Naph	2	$N(CH_2)_2COOH$	CH_2	17	-
16	Naph	2	$N(CH_2)_2CH_2OH$	CH_2	59	27.0±5.7 μM
18	Naph	2	$N(CH_2)_3COOH$	CH_2	40	-
19	Naph	2	$N(CH_2)_3CH_2OH$	CH_2	82	7.0±2.18 μM
21	Naph	2	$N(CH_2)_4COOH$	CH_2	49	-
22	Naph	2	$N(CH_2)_4CH_2OH$	CH_2	71	10.5±1 μM
23	Naph	1	NH	CH_2	88	34.5±2.5 μM
25	Naph	1	$N(CH_2)_2COOH$	CH_2	70	28.4±4.7 μM
26	Naph	1	$N(CH_2)_2CH_2OH$	CH_2	73	20.5±0.65 μM
28	Naph	1	$N(CH_2)_3COOH$	CH_2	44	-
29	Naph	1	$N(CH_2)_3CH_2OH$	CH_2	85	33.8±0.4 μM
31	Naph	1	$N(CH_2)_4COOH$	CH_2	8	-
32	Naph	1	$N(CH_2)_4CH_2OH$	CH_2	68	23.0±0.9 μM

[a]Efficacy has been calculated in transactivation assay on HepG2 cells as percent of inhibition of transactivation caused by CDCA at 10 μM, set as 100%. [b]IC_{50} has been determined for efficacy ≥50%. IC_{50} values (μM) were calculated from at least three experiments. Results are expressed as mean ± SEM.

All the synthesized compounds showed no agonistic activity toward FXR (Figure S3).

The efficacy of compounds **3f** and **13** on FXR was then evaluated in a cell-free SRC-1 recruitment Alpha Screen experiment. In this assay, FXR-SRC-1 recruitment is measured in the presence of CDCA at 500 nM with or without different concentrations of **3f** and **13**. As reported in Figure 2A, both compounds show high efficacy in counteracting SRC-1 peptide recruitment prompted by CDCA when tested at 500 and 1000 nM. Afterward, we attempted to see whether **3f** and **13** interacts with common off-targets, such as the nuclear receptors liver X receptor α and β (LXRα and -β), the

DOI: 10.1021/acsmedchemlett.8b00534
ACS Med. Chem. Lett. 2019, 10, 504−510

Scheme 1. General Synthetic Procedure To Prepare 1,2,4-Oxadiazole Derivatives 3a−f[a]

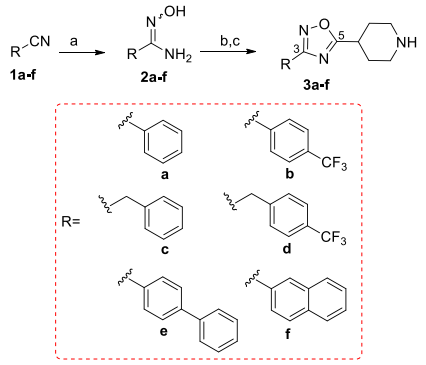

[a]Reagents and conditions: (a) NH_2OH HCl, K_2CO_3 in CH_3OH, reflux, 100−90% yield; (b) *N*-Boc-Inp-OH, DIPEA, HBTU in DMF dry, 80 °C, 60−80% yield; (c) TFA/CH_2Cl_2 1:1, 2 h, quantitative yield.

Scheme 2. Synthesis of Analogues 4−32[a]

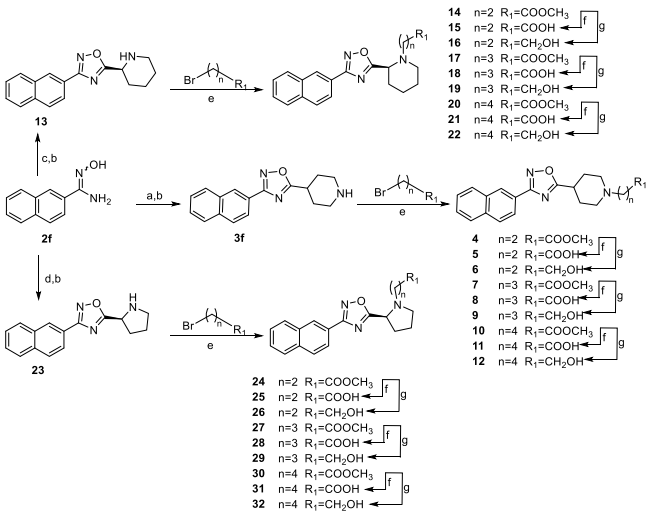

[a]Reagents and conditions: (a) *N*-Boc-Inp-OH, DIPEA, HBTU in DMF, 80 °C, 80% yield; (b) TFA/CH_2Cl_2 1:1, 2 h, quantitative yield; (c) *N*-Boc-L-Pip-OH, DIPEA, HBTU in DMF dry, 80 °C, 78% yield; (d) *N*-Boc-L-Pro-OH, DIPEA, HBTU in DMF dry, 80 °C, 83% yield; (e) methyl 3-bromopropanoate, methyl 4-bromobutanoate, or methyl 5-bromopentanoate, DIPEA, in CH_3CN dry, 60 °C, overnight, 65−92% yield; (f) LiOH in THF/H_2O (2:1), 0 °C then room temperature, 24 h, 40−60% yield; (g) DIBAL-H (1 M in toluene) in THF dry, 0 °C, 48 h, 57−82% yield.

peroxisome proliferator-activated receptor γ (PPARγ), and pregnane X receptor (PXR) (Figure 2B,C). Compounds **3f** and **13** showed no agonistic and antagonistic effects toward any of these receptors.

In order to evaluate the physicochemical parameters of the above-mentioned analogs, LC-MS analysis was assessed (Table 2). Both compounds exhibited good aqueous solubility offering also the possibility to improve this property as well as their polarity by a salt formation via the amine group. Instead, large differences were observed in their metabolic stability, as resulted by in vitro incubation with rat liver microsomes. Compound **13** showed a very low metabolic stability in vitro, with only 9.4% of unmodified molecule remaining after 40 min, and these data rule out its pharmacological potential.

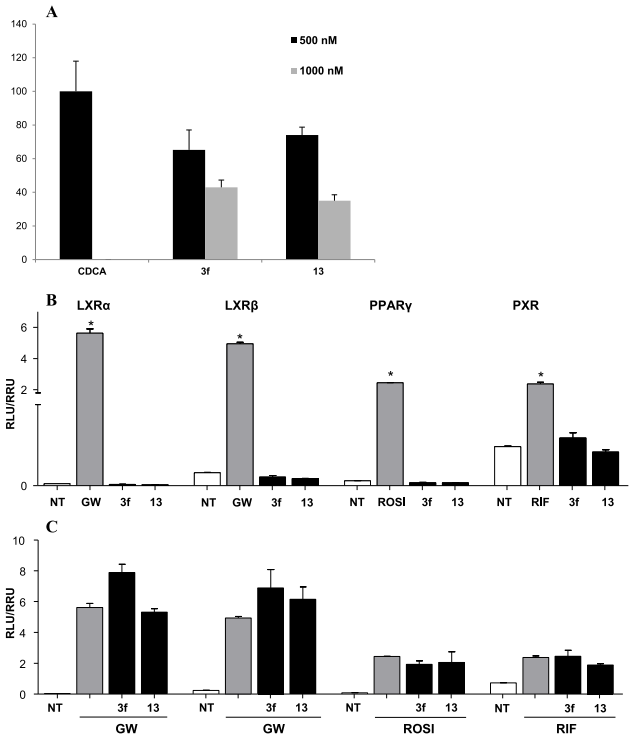

Figure 2. (A) Effect of **3f** and **13** at 500 and 1000 nM in antagonizing SRC-1 recruitment on FXR by CDCA at 500 nM. Each measurement has been repeated in triplicate and SD < 5%. (B, C) Off-target activity. (B) HepG2 cells were stimulated with GW3965 (GW, 10 μM) or Rosiglitazone (ROSI, 500 nM), or Rifaximin (RIF, 10 μM) as positive controls and compounds **3f** and **13** (10 μM); (C) cells were stimulated with 5 μM of compounds **3f** and **13** in combination with the relative positive control. Results are expressed as mean ± SEM. *p < 0.05 versus not treated cells (NT).

Table 2. In Vitro Pharmacokinetics for Compounds 3f and 13

compound	solubility[a] (μM)	log D	Cl_{int}[b]	$t_{1/2}$ (min)	%[c]
3f	200	0.34	20.67	111.8	76.2
13	110.4	0.58	201	11.5	9.4

[a]Aqueous solubility at pH 7.4. [b]Reported as μL/min/mg protein. [c]Percentage of compound remaining in solution after 40 min of incubation. Each measurement has been repeated in triplicate and SD < 5%.

Collectively, compound **3f** combines the high potency/efficacy in antagonizing FXR (Table 1) with excellent metabolic stability (about 76% remaining after 40 min of in vitro incubation, Table 2), thus representing a new promising chemotype of FXR antagonist. Furthermore, we also tested its behavior in the parallel artificial membrane permeability assay (PAMPA) to measure its effective permeability (expressed as log Pe) through an artificial lipid membrane.[17] Propanolol and furosemide at 250 μM were used as positive and negative control molecules giving a log Pe of −4.875 for propanolol and −6.503 for furosemide. In this assay, **3f** displayed an average propensity to cross the membrane in vitro (logPe −5.046).

To gain insights into the antagonism of compound **3f**, we then investigated the downstream genes of FXR by real-time PCR (Figure 3). The HepG2 (1×10^6) were plated and, after 24 hours of starvation, were stimulated with CDCA (10 μM) and compound **3f** at 0.1 and 1 μM concentration.

DOI: 10.1021/acsmedchemlett.8b00534
ACS Med. Chem. Lett. 2019, 10, 504−510

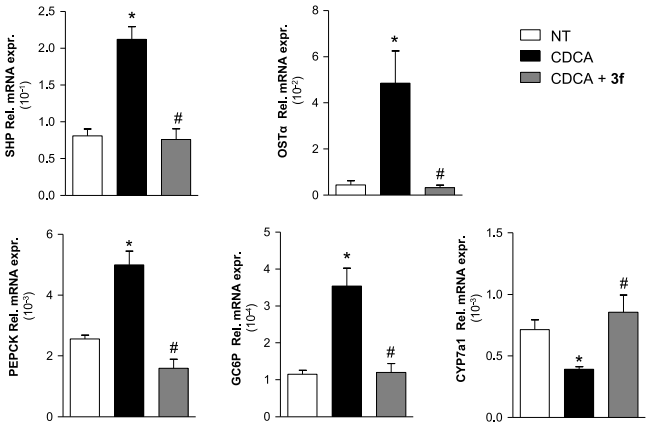

Figure 3. Compound **3f** modulates FXR target genes. Real-time PCR analysis of mRNA expression on FXR target genes in HepG2 cells primed with CDCA (10 μM) alone or in combination with increasing concentrations of **3f** (0.1 and 1 μM) or with vehicle (DMSO) alone. Values are normalized to GAPDH. The relative mRNA expression is analyzed according to the CT method. Data were calculated from at least three experiments. Results are expressed as actual mean between the two concentrations ± SEM. *p < 0.05 versus not treated cells (NT); #p < 0.05 versus CDCA stimulated cells.

As shown in Figure 3, CDCA induces the expression of SHP, OSTα, PEPCK, and GC6P whereas a decrease of CYP7A1 relative to mRNA expression and **3f** reverts the effect of CDCA on the above FXR targeted genes. These results demonstrate that compound **3f** is a potent, effective, and selective FXR antagonist.

In order to elucidate the binding mode of the newly synthesized FXR antagonists, we performed docking calculations, which is a widely used computational technique to generate and rank ligand/protein complexes based on empirical scoring functions.[18−20]

In particular, we performed molecular docking calculations on the most potent derivatives **3f** and **13** (Figure 4) in the crystal structure of the FXR-ligand binding domain (LBD) in the antagonistic conformation (PDB code: 4OIV).[21]

We note that the structure of the FXR-LBD in this conformation is rather different if compared with that of the FXR-LBD in the agonistic form. In particular, in the agonistic state, the ligand binding site is defined by helices 3, 5, 6, 7, 11, and 12, with the latter forming the recognition site for the coactivator peptides.[22] At variance with the agonistic form, in the antagonistic state, the hydrophobic C-terminal part of H11 is bent filling part of the ligand binding pocket and sending H12 to the binding site of the coactivators peptides of the other FXR monomer. This conformational change blocks the receptor in a not activable state.[21]

Docking of **3f** and **13** (lowest energy conformation, Figure 4) in the FXR-LBD antagonistic conformation shows that the ligand oxadiazole ring engages both a water-mediated hydrogen bond and a T-shape interaction with the side chain of His451 on H11. Additionally, the naphtyl ring of **3f** and **13** establishes a number of hydrophobic contacts with residues such as Ala295, Val299, Leu455, and Met456. On the other side, the piperidine ring of **3f** and **13** can establish favorable interactions with Ile356 and Ile361 and might form water-mediated hydrogen bonds with Ser336 and Tyr373. The overlap in the FXR-LBD of the binding mode of **3f** and **13** with that of the FXR cocrystallized antagonist *N*-benzyl-*N*-(3-(*tert*-butyl)-4-hydroxyphenyl)-2,6-dichloro-4-(dimethylamino)

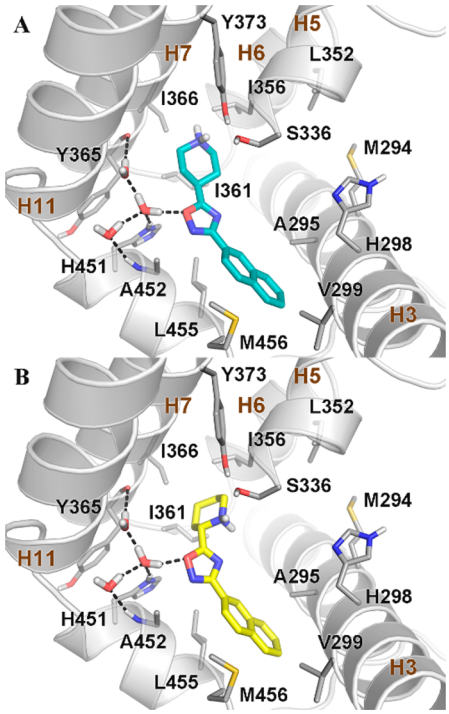

Figure 4. Docking pose of (A) **3f** (cyan sticks) and (B) **13** (yellow sticks) in the crystal structure of the FXR-LBD (PDB code: 4OIV).[21] FXR is shown as gray cartoons, with amino acids important for ligand binding depicted as sticks. Nonpolar hydrogens are omitted for clarity. Hydrogen bonds are shown as dashed black lines.

benzamide (NDB) shows that the ligands occupy similarly the ligand binding site, although NDB can form additional interactions with the receptor through its 3-(*tert*-butyl)-4-hydroxyphenyl moiety (Figure S1). Interestingly, additional docking calculations on **9** show that also the binding mode of this compound is superimposable to that of NBD (Figure S2). This finding explains why compounds endowed with an alcoholic side chain on the piperidine nucleus (i.e., **9**, **19**, **22**, and **26**) have an FXR antagonistic profile.

In conclusion, we report the discovery of a new chemotype of FXR antagonists, featuring a central oxadiazole ring with a protonable piperidine nucleus at C-5 and a naphtyl group at C-3. We note that the piperidine moiety plays a different role in our compounds if compared with the compounds reported by Teno et al.[13] In particular, in the Teno's compounds, the piperidine works as a spacer to place the H-bond acceptor group (the carbonyl CO) in the proper position to interact with His298, while in our compounds, the piperidine is not acetylated and therefore available as H-bond donor group in the FXR-LBD. Furthermore, the presence of a free piperidine makes our compounds basic with the piperidine protonated and an overall net charge equal to +1.

Our study identified compounds **3f** and **13** as potent and selective FXR antagonists. The ability in reverting the effect of CDCA on the expression of several FXR targeted genes combined with the excellent pharmacokinetic properties makes compound **3f** the most promising lead identified in this study and suitable for further development.

DOI: 10.1021/acsmedchemlett.8b00534
ACS Med. Chem. Lett. 2019, 10, 504−510

■ ASSOCIATED CONTENT

Supporting Information

The Supporting Information is available free of charge on the ACS Publications website at DOI: 10.1021/acsmedchemlett.8b00534.

Experimental procedures; docking poses of **3f** and **13** with the crystallographic pose of NBD at the FXR-LBD; docking pose of **9** and its superposition with the crystallographic pose of NBD at the FXR-LBD; FXR transactivation on HepG2 cells; ^{1}H NMR of compounds **3a**−**3f** and **4**−**32** (PDF)

■ AUTHOR INFORMATION

Corresponding Author

*E-mail: sidemari@unina.it.

ORCID

Maria Chiara Monti: 0000-0002-1337-2909
Angela Zampella: 0000-0002-6170-279X
Simona De Marino: 0000-0002-0300-5048

Funding

This work was supported by University of Naples Federico II "Finanziamento della Ricerca in Ateneo (DR/2016/341, February 2016)", by MIUR-ITALY PRIN2015 "Top-down and Bottom-up approach in the development of new bioactive chemical entities inspired on natural products scaffolds" (Project N. 2015MSCKCE_003), and by the Swiss National Science Foundation (Project N. 200021_163281). V.L. also thanks the COST action CA15135 (Multitarget paradigm for innovative ligand identification in the drug discovery process MuTaLig) for the support.

Notes

The authors declare no competing financial interest.

■ ABBREVIATIONS

AF-2, activation function 2 (domain); Boc, *tert*-butyloxycarbonyl; CDCA, chenodeoxycholic acid; Cl_{int}, intrinsic clearance; CYP7A1, cholesterol 7 α-hydroxylase; DIPEA, *N,N*-diisopropylethylamine; DMF, *N,N*-dimethylformamide; 6-ECDCA, 6-ethyl chenodeoxycholic acid; FXR-LBD, Farnesoid X Receptor−Ligand Binding Domain; HBTU, *N,N,N′,N′*-tetramethyl-*O*-(1*H*-benzotriazol-1-yl)uronium hexafluorophosphate; NAFLD, nonalcoholic fatty liver disease; GC6P, glucose-6-phosphatase; NDB, *N*-benzyl-*N*-(3-(*tert*-butyl)-4-hydroxyphenyl)-2,6-dichloro-4-(dimethylamino) benzamide; OSTα, organic solute transporter α; PAMPA, parallel artificial membrane permeability assay; PCR, polymerase chain reaction; PDB, protein data bank; PEPCK, phosphoenolpyruvate carboxykinase; SHP, small heterodimer partner; SRC-1, steroid receptor coactivator-1; TFA, trifluoroacetic acid

■ REFERENCES

(1) Forman, B. M.; Goode, E.; Chen, J.; Oro, A. E.; Bradley, D. J.; Perlmann, T.; Noonan, D. J.; Burka, L. T.; McMorris, T.; Lamph, W. W.; Evans, R. M.; Weinberger, C. Identification of a nuclear receptor that is activated by farnesol metabolites. *Cell* **1995**, *81*, 687−693.

(2) Makishima, M.; Okamoto, A. Y.; Repa, J. J.; Tu, H.; Learned, R. M.; Luk, A.; Hull, M. V.; Lustig, K. D.; Mangelsdorf, D. J.; Shan, B. Identification of a nuclear receptor for bile acids. *Science* **1999**, *284*, 1362−1365.

(3) Parks, D. J.; Blanchard, S. G.; Bledsoe, R. K.; Chandra, G.; Consler, T. G.; Kliewer, S. A.; Stimmel, J. B.; Willson, T. M.; Zavacki, A. M.; Moore, D. D.; Lehmann, J. M. Bile acids: natural ligands for an orphan nuclear receptor. *Science* **1999**, *284*, 1365−1368.

(4) Zhang, Y.; Lee, F. Y.; Barrera, G.; Lee, H.; Vales, C.; Gonzalez, F. J.; Willson, T. M.; Edwards, P. A. Activation of the nuclear receptor FXR improves hyperglycemia and hyperlipidemia in diabetic mice. *Proc. Natl. Acad. Sci. U. S. A.* **2006**, *103*, 1006−1011.

(5) Claudel, T.; Staels, B.; Kuipers, F. The farnesoid X receptor: a molecular link between bile acid and lipid and glucose metabolism. *Arterioscler., Thromb., Vasc. Biol.* **2005**, *25*, 2020−2030.

(6) Cipriani, S.; Mencarelli, A.; Palladino, G.; Fiorucci, S. FXR activation reverses insulin resistance and lipid abnormalities and protects against liver steatosis in Zucker (fa/fa) obese rats. *J. Lipid Res.* **2010**, *51*, 771−784.

(7) Brzozowski, A. M.; Pike, A. C.; Dauter, Z.; Hubbard, R. E.; Bonn, T.; Engström, O.; Ohman, L.; Greene, G. L.; Gustafsson, J. A.; Carlquist, M. Molecular basis of agonism and antagonism in the oestrogen receptor. *Nature* **1997**, *389*, 753−758.

(8) Prawitt, J.; Caron, S.; Staels, B. How to modulate FXR activity to treat the metabolic syndrome. *Drug Discovery Today: Dis. Mech.* **2009**, *6*, e55−e64.

(9) Cariou, B.; Staels, B. FXR: a promising target for the metabolic syndrome? *Trends Pharmacol. Sci.* **2007**, *28*, 236−243.

(10) Sepe, V.; Distrutti, E.; Fiorucci, S.; Zampella, A. Farnesoid X receptor modulators 2014-present: a patent review. *Expert Opin. Ther. Pat.* **2018**, *28*, 351−364.

(11) Stedman, C.; Liddle, C.; Coulter, S.; Sonoda, J.; Alvarez, J. G.; Evans, R. M.; Downes, M. Benefit of farnesoid X receptor inhibition in obstructive cholestasis. *Proc. Natl. Acad. Sci. U. S. A.* **2006**, *103*, 11323−11328.

(12) Xu, Y. Recent progress on bile acid receptor modulators for treatment of metabolic diseases. *J. Med. Chem.* **2016**, *59*, 6553−6579.

(13) Teno, N.; Yamashita, Y.; Iguchi, Y.; Fujimori, K.; Une, M.; Nishimaki-Mogami, T.; Hiramoto, T.; Gohda, K. Nonacidic chemotype possessing N-acylated piperidine moiety as potent farnesoid *X* receptor (FXR) antagonists. *ACS Med. Chem. Lett.* **2018**, *9*, 78−83.

(14) Schmidt, J.; Schierle, S.; Gellrich, L.; Kaiser, A.; Merk, D. Structural optimization and in vitro profiling of *N*-phenylbenzamide-based farnesoid X receptor antagonists. *Bioorg. Med. Chem.* **2018**, *26*, 4240−4253.

(15) Gonzalez, F. J.; Jiang, C.; Patterson, A. D. An intestinal microbiota-farnesoid X receptor axis modulates metabolic disease. *Gastroenterology* **2016**, *151*, 845−59.

(16) Flesch, D.; Gabler, M.; Lill, A.; Carrasco Gomez, R.; Steri, R.; Schneider, G.; Stark, H.; Schubert-Zsilavecz, M.; Merk, D. Fragmentation of GW4064 led to a highly potent partial farnesoid X receptor agonist with improved drug-like properties. *Bioorg. Med. Chem.* **2015**, *23*, 3490−3498.

(17) Miele, E.; Valente, S.; Alfano, V.; Silvano, M.; Mellini, P.; Borovika, D.; Marrocco, B.; Po, A.; Besharat, Z.; Catanzaro, G.; Battaglia, G.; Abballe, L.; Zwergel, C.; Stazi, G.; Milite, C.; Castellano, S.; Tafani, M.; Trapencieris, P.; Mai, A.; Ferretti, E. The histone methyltransferase EZH2 as a druggable target in SHH medulloblastoma cancer stem cells. *Oncotarget* **2017**, *8*, 68557−68570.

(18) Anzini, M.; Braile, C.; Valenti, S.; Cappelli, A.; Vomero, S.; Marinelli, L.; Limongelli, V.; Novellino, E.; Betti, L.; Giannaccini, G.; Lucacchini, A.; Ghelardini, C.; Norcini, M.; Makovec, F.; Giorgi, G.; Ian Fryer, R. Ethyl 8-Fluoro-6-(3-nitrophenyl)-4H-imidazo[1,5-a]-[1,4]benzodiazepine-3-carboxylate as novel, highly potent, and safe antianxiety agent. *J. Med. Chem.* **2008**, *51*, 4730−4743.

(19) Famiglini, V.; La Regina, G.; Coluccia, A.; Pelliccia, S.; Brancale, A.; Maga, G.; Crespan, E.; Badia, R.; Riveira-Muñoz, E.; Esté, J. A.; Ferretti, R.; Cirilli, R.; Zamperini, C.; Botta, M.; Schols, D.; Limongelli, V.; Agostino, B.; Novellino, E.; Silvestri, R. Indolylarylsulfones carrying a heterocyclic tail as very potent and broad spectrum HIV-1 non-nucleoside reverse transcriptase inhibitors. *J. Med. Chem.* **2014**, *57*, 9945−9957.

(20) Nuti, E.; Casalini, F.; Avramova, S. I.; Santamaria, S.; Fabbi, M.; Ferrini, S.; Marinelli, L.; La Pietra, V.; Limongelli, V.; Novellino, E.; Cercignani, G.; Orlandini, E.; Nencetti, S.; Rossello, A. Potent

DOI: 10.1021/acsmedchemlett.8b00534
ACS Med. Chem. Lett. 2019, 10, 504−510

arylsulfonamide inhibitors of tumor necrosis factor-α converting enzyme able to reduce activated leukocyte cell adhesion molecule shedding in cancer cell models. *J. Med. Chem.* **2010**, *53*, 2622−2635.
(21) Xu, X.; Xu, X.; Liu, P.; Zhu, Z. Y.; Chen, J.; Fu, H. A.; Chen, L. L.; Hu, L. H.; Shen, X. Structural basis for small molecule NDB (*N*-Benzyl-*N*-(3-(tert-butyl)-4-hydroxyphenyl)-2,6-dichloro-4-(dimethylamino) benzamide) as a selective antagonist of farnesoid X receptor α (FXR α) in stabilizing the homodimerization of the receptor. *J. Biol. Chem.* **2015**, *290*, 19888−19899.
(22) Mi, L. Z.; Devarakonda, S.; Harp, J. M.; Han, Q.; Pellicciari, R.; Willson, T. M.; Khorasanizadeh, S.; Rastinejad, F. Structural basis for bile acid binding and activation of the nuclear receptor FXR. *Mol. Cell* **2003**, *11*, 1093−1100.

DOI: 10.1021/acsmedchemlett.8b00534
ACS Med. Chem. Lett. 2019, 10, 504−510